ISSN 1330-3651 (Print), ISSN 1848-6339 (Online)
DOI: 10.17559/TV-20150328135652

FAULT DIAGNOSTICS OF ACOUSTIC SIGNALS OF LOADED SYNCHRONOUS MOTOR USING SMOFS-25-EXPANDED AND SELECTED CLASSIFIERS

Adam Glowacz

Original scientific paper
A system of fault diagnostics of loaded synchronous motor was proposed. Proposed system was based on acoustic signals of loaded synchronous motor. A new method of feature extraction SMOFS-25-EXPANDED (shorted method of frequencies selection-25-Expanded) was proposed. Presented method was analysed for 3 classifiers: LDA (Linear Discriminant Analysis), NN (Nearest Neighbour), SOM (Self-organizing Map). Analysis was carried out for real incipient states of loaded synchronous motor. Acoustic signals generated by motor were used in analysis. The following states of motor were analysed: healthy motor, motor with shorted stator coil, motor with shorted stator coil and broken coil, motor with shorted stator coil and two broken coils. These states are caused by natural degradation of rotating synchronous motor. The results of recognition were good. Proposed method of acoustic signal recognition can be used to protect loaded synchronous motors.

Keywords: *acoustic signal; fault detection; loaded synchronous motor; recognition*

Dijagnostika greške akustičkih signala opterećenog sinkronog motora primjenom SMOFS-25-EXPANDED i odabranih klasifikatora

Izvorni znanstveni članak
Predlaže se sustav dijagnostike greške opterećenog sinkronog motora. Predloženi se sustav zasniva na akustičkim signalima opterećenog sinkronog motora. Predlaže se nova metoda određivanja karakteristika SMOFS-25-EXPANDED (shorted method of frequencies selection-25-expaned – skraćena metoda za izbor frekvencija-25-proširena). Predložena se metoda analizirala u odnosu na tri klasifikatora: LDA (Linear Discriminant Analysis – analiza linearnog diskriminatora), NN (Nearest Neighbour – najbliži susjed), SOM (Self-organizing Map – samoorganizirajuća mapa). Analiza je provedena za stvarno početna stanja opterećenog sinkronog motora. U analizi su iskorišteni akustički signali koje je stvarao motor. Analizirala su se sljedeća stanja motora: ispravan motor, motor sa skraćenim namotajem statora, motor sa skraćenim namotajem statora i prekinutim namotajem, motor sa skraćenim namotajem statora i dva prekinuta namotaja. Do takvih je stanja došlo zbog prirodne degradacije rotirajućeg sinkronog motora. Rezultati analize su dobri. Predložena metoda prepoznavanja akustičkog signala može se primijeniti za zaštitu opterećenih sinkronih motora.

Ključne riječi: *akustički signal; otkrivanje greške; opterećeni sinkroni motor; priznanje*

1 Introduction

One of the types of AC motors is synchronous motor. The synchronous motors behave as constant speed motor. They are independent of load condition. The synchronous motors can be used for: line shafts, blowers, compressors, reciprocating pumps, centrifugal pumps and paper mills. At the end of transmission lines, these types of motors are used to regulate the voltage. Moreover synchronous motors are used with variable frequency drive system, by that meaning that wide range of speeds can be obtained in metallurgy industry [1].

The performance of the synchronous motor depends on the structure of electric circuit. Moreover it depends on the type of material and its treatment [2÷5].

To diagnose electric motor many methods were proposed in the literature. Some of them are based on recognition of electric, vibro-acoustic, thermal signals [6÷27]. Most of them are based on electric signals, because these signals are not disturbed so much as acoustic signals [1, 8, 10, 56]. The methods based on acoustic signals are not known in the literature. Moreover these methods are non-invasive and inexpensive. Microphone and computer cost about 300 $.

The system of detection of predefined incipient faults is employed as a tool to protect the synchronous motors (Fig. 1). The most important profit of the system is that the probable fault of the synchronous motor can be predicted [25]. Moreover incipient faults of motor may cause production and operation shutdowns. These shutdowns may cause waste of money, production time, resources and employee time.

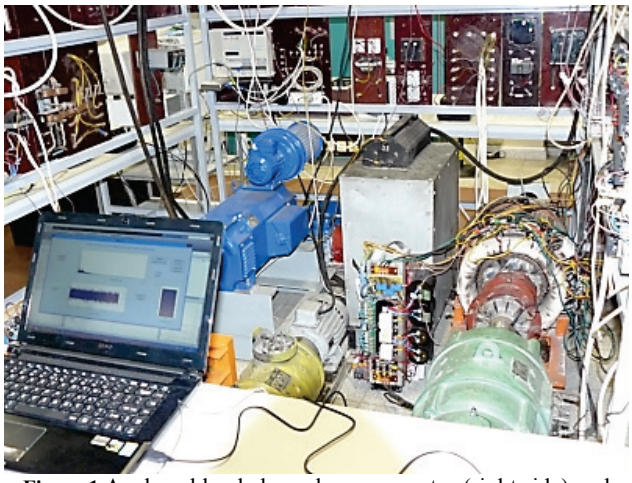

Figure 1 Analyzed loaded synchronous motor (right side) and system of fault diagnostics (left side)

This paper describes a new method of diagnostics of the loaded synchronous motor. The paper is organized in 4 sections. Section 1 describes applications of rotating synchronous motors and method of diagnostics of electrical motors. Presented method of recognition of acoustic signal of rotating synchronous motor is developed in Section 2. The new method of feature extraction SMOFS-25-EXPANDED is also presented in Section 2. Analysis of acoustic signal of loaded synchronous motor is described in Section 3. The paper is

summarized in Section 4 along with the plan of future researches.

2 Presented method of recognition of acoustic signal of rotating synchronous motor

The presented method of recognition is showed in Fig. 2. It has 6 steps of processing. Step 1 is the recording of acoustic signal of loaded synchronous motor. Capacitor microphone and a notebook computer are used to record acoustic signal. Various microphones can be used in this step. Step 2 is splitting the recorded soundtrack into small samples. Step 3 is normalization of the amplitude of the obtained small samples. Step 4 is calculation of FFT spectrum. Step 5 is calculation of SMOFS-25-EXPANDED algorithm. Step 6 consists of 2 substeps – Steps 6a, 6b. Step 6a is calculation of patterns (training samples). Step 6b is calculation of results (test samples).

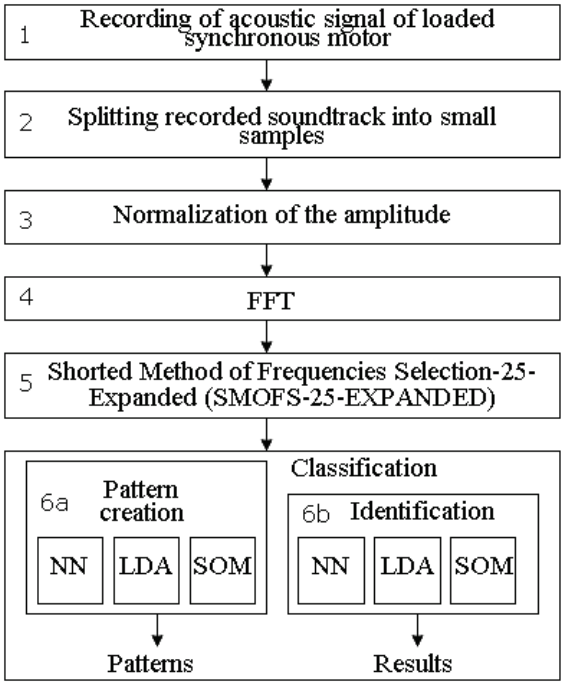

Figure 2 Presented method of recognition of acoustic signal of rotating synchronous motor using FFT, SMOFS-25-EXPANDED, NN, LDA and SOM

2.1 Recording of acoustic signal

Capacitor microphone and a notebook computer are used to record acoustic signal of loaded synchronous motor [28]. This soundtrack has the following parameters: mono, 44100 Hz, 16-bit depth, WAVE PCM.

2.2 Pre-processing

Pre-processing of acoustic signal consists of 3 steps: splitting recorded soundtrack into 5-seconds samples, normalization of the amplitude, calculation of FFT [8]. Hamming window with the length of 32 768 is used to calculate 16 384 elements of FFT spectrum (32 768/44 100=0,743, duration of 1 window equals 0,743 s).

2.3 Shorted method of frequencies selection-25-Expanded

In the literature many feature extraction methods are described. In this subsection, author proposes method of feature extraction of loaded synchronous motor - SMOFS-25-EXPANDED. Presented method uses differences between amplitudes of frequencies of states of the loaded synchronous motor. Healthy and faulty states of the loaded synchronous motor generate different acoustic signals. Steps of SMOFS-25-EXPANDED method are described below:

1. Calculate the FFT spectrum of acoustic signal for each state of loaded synchronous motor. The FFT spectrum of acoustic signal of healthy state of loaded synchronous motor is expressed by vector $\boldsymbol{h} = [h_1, h_2, ..., h_{16384}]$. The FFT spectrum of acoustic signal of loaded synchronous motor with shorted stator coil is expressed by vector $\boldsymbol{ss} = [ss_1, ss_2, ..., ss_{16384}]$. The FFT spectrum of acoustic signal of loaded synchronous motor with shorted stator coil and broken coil is expressed by vector $\boldsymbol{ssbc} = [ssbc_1, ssbc_2, ..., ssbc_{16384}]$. The FFT spectrum of acoustic signal of loaded synchronous motor with shorted stator coil and two broken coils is expressed by vector $\boldsymbol{sstbc} = [sstbc_1, sstbc_2, ..., sstbc_{16384}]$.
2. Calculate differences between FFT spectra of acoustic signals of states of loaded synchronous motor: ***h-ss***, ***h-ssbc***, ***h-sstbc***, ***ss-ssbc***, ***ss-sstbc***, ***ssbc-sstbc***.
3. Calculate absolute values of differences between FFT spectra of acoustic signals of states of loaded synchronous motor: |***h-ss***|, |***h-ssbc***|, |***h-sstbc***|, |***ss-ssbc***|, |***ss-sstbc***|, |***ssbc-sstbc***|.
4. Select the frequencies, which meet the following criterion:

$$||AFS_1| - |AFS_2|| > TOS, \tag{1}$$

where TOS – threshold of selection of amplitudes of frequencies (formula 1), $||AFS_1| - |AFS_2||$ – the difference of amplitudes of frequencies for states 1 and 2 of the motor, AFS_1 - amplitude of frequency of state 1 of the motor, AFS_2 - amplitude of frequency of state 2 of the motor.

5. TOS is calculated according to the following formulas (2) and (3):

$$TOS = \frac{\sum_{NF=1}^{NF} || AFS_1 | - | AFS_2 ||}{NF}, \tag{2}$$

$$NF \leq 25, \tag{3}$$

If the parameter NF is greater than 25, SMOFS-25-EXPANDED does loop calculations (formula 2). If NF is smaller or equal to 25 it finishes its calculations. NF – number of frequencies (initially NF =16 384, because FFT method gives 16384 frequencies for window length 32 768. SMOFS-25-EXPANDED calculates feature vector with 1-25 features. The number of features depends on the number of analysed states, type of fault and external noises. There is a possibility that the differences between amplitudes of frequencies of two states may

have various values. For example SMOFS-25-EXPANDED selects frequencies 110, 220, 330, 440, 550 Hz for states A and B. SMOFS-25-EXPANDED selects frequencies 110, 230, 340, 450, 560 Hz for states A and C. SMOFS-25-EXPANDED selects frequencies 120, 220, 340, 460, 570 Hz for states B and C. It can be noticed that none of the frequencies is good for recognition of states A, B, C because selected frequency should be common for A and B, A and C, B and C. Frequencies 110, 220, 340 Hz are the best for recognition in this case. The proposed method should make decision about selection of frequencies. In this aim parameter *TE* is introduced.

6. Select parameter *TE* = (*number of required common frequencies*)/(*number of all selected frequencies*). This parameter defines how many common frequencies are selected. For example, when *TE* is equal to 0,665, then 2 of 3 frequencies are required ((2/3) > 0,665) to make decision about common frequencies (see example above). In the mentioned example 110, 220, 340 Hz are selected for *TE* = 0,665. If parameter *TE* is equal to 0,668 ((2/3) < 0,668), none of frequencies will be selected.
7. Select these amplitudes of selected frequencies and form feature vector.

A block diagram of the shorted method of frequencies selection-25-Expanded is showed in Fig. 3.

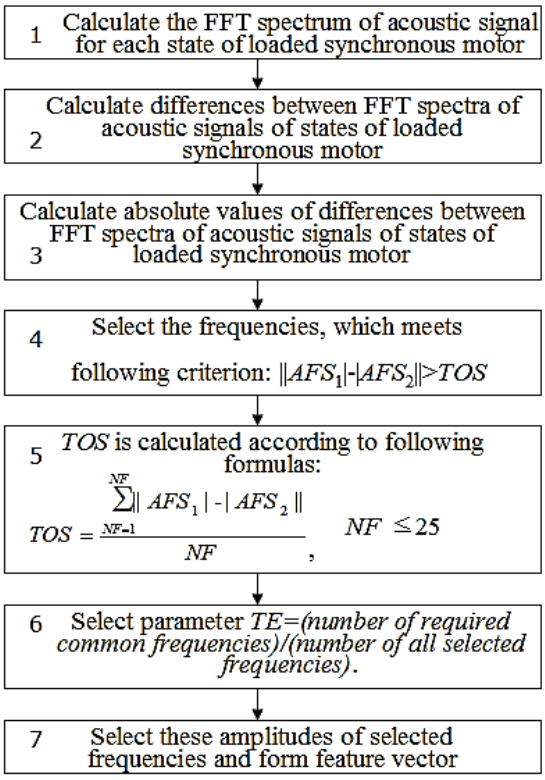

Figure 3 Block diagram of SMOFS-25-EXPANDED

Differences between FFT spectra of analysed states of loaded synchronous motor with rotor speed 1500 rpm are presented in Figs. 4 ÷ 9.

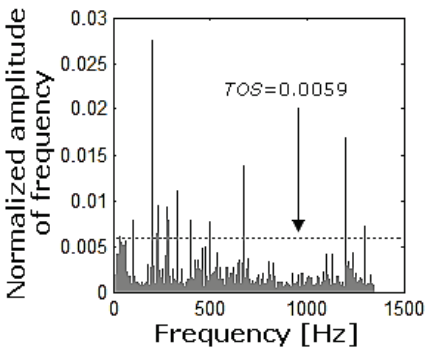

Figure 4 The difference between FFT spectra of acoustic signal of healthy state of loaded synchronous motor and acoustic signal of loaded synchronous motor with shorted stator coil (|***h-ss***|) and the obtained threshold by SMOFS-25-EXPANDED

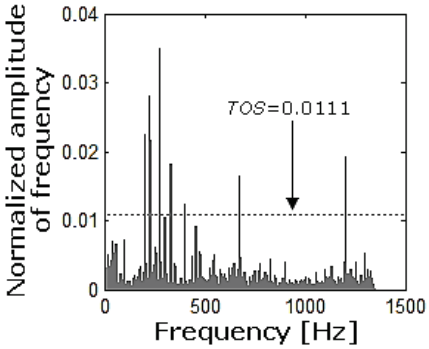

Figure 5 The difference between FFT spectra of acoustic signal of healthy state of loaded synchronous motor and acoustic signal of loaded synchronous motor with shorted stator coil and broken coil (|***h-ssbc***|) and the obtained threshold by SMOFS-25-EXPANDED

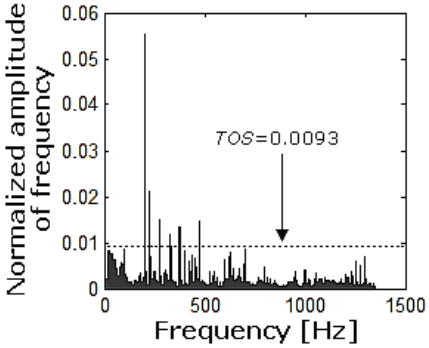

Figure 6 The difference between FFT spectra of acoustic signal of healthy state of loaded synchronous motor and acoustic signal of loaded synchronous motor with shorted stator coil and two broken coils (|***h-sstbc***|) and the obtained threshold by SMOFS-25-EXPANDED

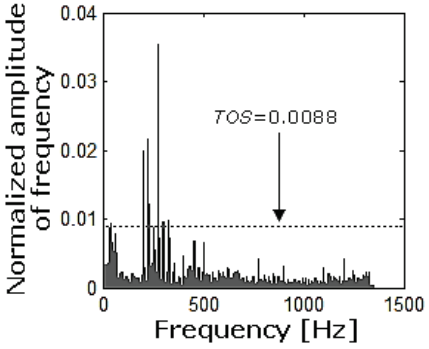

Figure 7 The difference between FFT spectra of acoustic signal of loaded synchronous motor with shorted stator coil and acoustic signal of loaded synchronous motor with shorted stator coil and broken coil (|***ss-ssbc***|) and the obtained threshold by SMOFS-25-EXPANDED

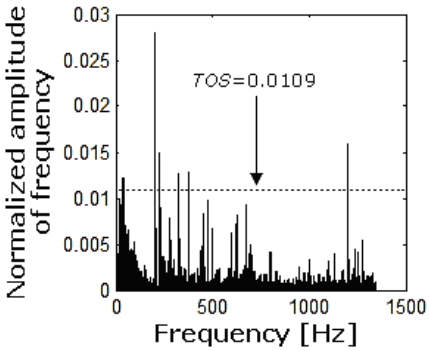

Figure 8 The difference between FFT spectra of acoustic signal of loaded synchronous motor with shorted stator coil and acoustic signal of loaded synchronous motor with shorted stator coil and two broken coils (|***ss-sstbc***|) and the obtained threshold by SMOFS-25-EXPANDED

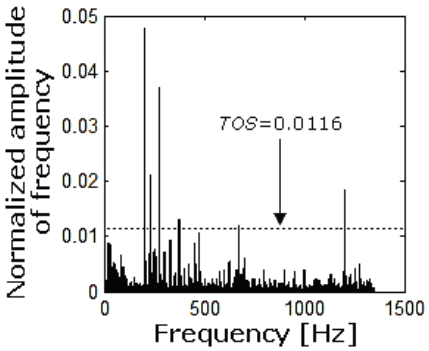

Figure 9 The difference between FFT spectra of acoustic signal of loaded synchronous motor with shorted stator coil and broken coil and acoustic signal of loaded synchronous motor shorted stator coil and two broken coils (|***ssbc-sstbc***|) and the obtained threshold by SMOFS-25-EXPANDED

Each training set contained 4 training samples. Two training sets were used in analysis (see Section 3). Selection of common frequencies of 4 states of loaded synchronous motor depending on parameter *TE* and training sets was shown in Tab. 1.

Table 1 Selection of common frequencies of 4 states of loaded synchronous motor depending on parameter *TE* and training sets

TE = 0,99	Frequency (Hz)
Training set 1	--
Training set 2	--
Common frequencies	--
TE = 0,83	Frequency (Hz)
Training set 1	200
Training set 2	200, 202, 226, 276, 278
Common frequencies	200
TE = 0,65	Frequency (Hz)
Training set 1	200, 203, 226, 276, 277, 1198
Training set 2	200, 202, 226, 276, 207, 278
Common frequencies	200, 226, 276

Amplitudes of common frequencies of 4 states of loaded synchronous motor formed feature vectors (amplitudes of the following frequencies: 200 Hz or 200, 226, 276 Hz). Obtained vectors were used by classification methods in the classification step.

2.4 Linear discriminant analysis

Classification is the last step of signal processing. This step is described as supervised learning techniques. Classifier predicts the class of a new unlabelled observation (test sample). Classification methods are developed in the literature [29 ÷ 57]. Many of them can be used for recognition of acoustic signals. A Linear Discriminant Analysis classifier (LDA) analyses data. Assume we have a set of D-dimensional samples x_1, x_2, x_3,..., x_N, N_1 of which belongs to class w_1, and N_2 to class w_2. We want to obtain a scalar y by projecting the samples x onto a line $y=w^{\mathrm{T}}x$. Next we select the line that maximizes the separability of the scalars. A measure of separation is defined as the mean. The mean vector of each class in x-space and y-space is expressed by (4):

$$u_i = \frac{1}{N}\sum_{x\in w_i} x\,, \quad \tilde{u}_i = \frac{1}{N}\sum_{y\in w_i} y = w^{\mathrm{T}}u_i\,. \tag{4}$$

LDA method maximizes the difference between the means. Next it is normalized by a measure of the within-class scatter. The scatter is defined as:

$$\tilde{s}_i^2 = \sum_{y\in w_i}(y-\tilde{u}_i)^2. \tag{5}$$

The within-class scatter is defined as (6):

$$\tilde{s}_1^2 + \tilde{s}_2^2\,. \tag{6}$$

LDA maximizes the criterion function $J(w)$ expressed by:

$$J(w) = \frac{|\tilde{u}_1 - \tilde{u}_2|}{\tilde{s}_1^2 + \tilde{s}_2^2}. \tag{7}$$

In this way the training examples from the same class are projected close to each other. Moreover the obtained means are as farther apart as it is possible. More information about LDA classifier is available in the literature [8, 29, 38, 53].

2.5 Nearest neighbour

A nearest neighbour classifier is a technique for classification of different classes. The categorization of a new test sample is determined by the labels of the most similar already existing training sample. The NN classifier can be improved by distance functions such as: Manhattan, Euclidean, Minkowski, Jaccard distance. The NN classifier is the following:

1) For each sample S in the test set calculate the distance (S, G) between S and every sample G in the training set,
2) Neighbourhood contains the 1 neighbour in the training set closest to S,
3) On the basis of neighbourhood, select class for sample S [39].

Euclidean distance was used for the Nearest Neighbour classifier [11, 29].

2.6 Self-organizing map

A self-organizing map (SOM) is a method that uses unsupervised learning to create a map on a two-dimensional (training step). The location of points on the two-dimensional map shows the similarity between the considered points. This method is motivated by the observation of the operation of the biological brain. The SOM contains two steps: training and identification (mapping). Training samples are used to build the map. Test samples are used in identification step. The SOM consists of nodes. Nodes have weight vectors, which may be initialized randomly (similar to artificial neural network). Weight vectors are of the same dimension as the training vectors. To implement the SOM author uses Matlab Neural network toolbox [29]. More about the SOM and its learning algorithm can be found in the literature [40, 41].

3 Analysis of acoustic signals of loaded synchronous motor

Analysed loaded synchronous motor is presented in Fig. 1. Considered motor was loaded by the resistance R_{LO} = 1 Ω. All acoustic signals were recorded for rotor speed of 1500 rpm. This speed was also constant for fault states. Broken coils and short circuit were located in the stator circuit of the analysed motor (Fig. 10 ÷ 12). The resistance R_{SHCI} = 0,85 Ω was used for short-circuit of stator coils. Electrical parameters of loaded synchronous motor were depending on analysed states. These parameters were measured for each analysed state of machine:

- healthy loaded synchronous motor, I_{PHT} = 44,9 A, I_{LO} = 10 A, U_{PHRS} = 150 V (Fig. 13),
- loaded synchronous motor with shorted stator coil (B1-B2), I_{PHT} = 42,7 A, I_{LO} = 10 A, I_{SH} = 42,5 A, U_{PHRS} = 150 V,
- loaded synchronous motor with shorted stator coil (B1-B2) and broken coil (C2-C3), I_{PHT} = 47,2 A, I_{LO} = 10 A, I_{SH} = 38,8 A, U_{PHRS} = 150 V,
- loaded synchronous motor with shorted stator coil (B1-B2) and two broken coils (C2-C3, E2-E3), I_{PHT} = 32,3 A, I_{LO} = 10 A, I_{SH} = 32 A, U_{PHRS} = 150 V,

where I_{LO} - current of load, I_{PHT} - current of phase T, U_{PHRS} - voltage between phases R and S, I_{SH} - current of short circuit.

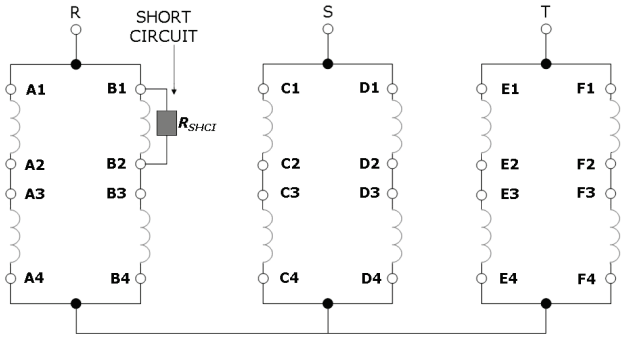

Figure 10 Scheme of shorted stator coil (B1-B2) of loaded synchronous motor

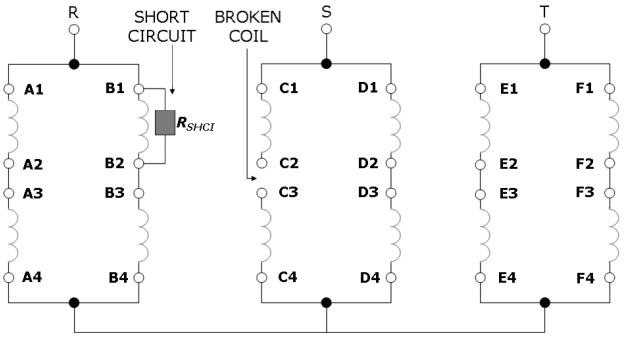

Figure 11 Scheme of shorted stator coil (B1-B2) and broken coil (C2-C3) of loaded synchronous motor

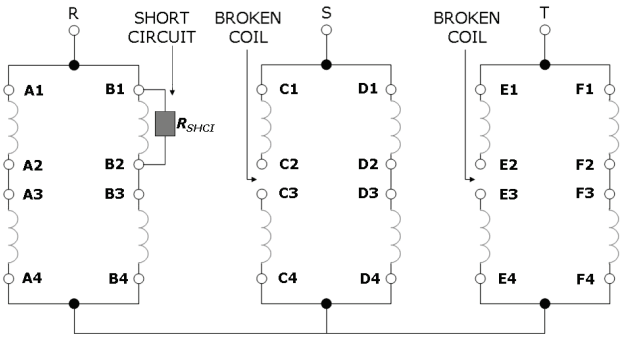

Figure 12 Scheme of shorted stator coil (B1-B2) and two broken coils (C2-C3, E2-E3) of loaded synchronous motor

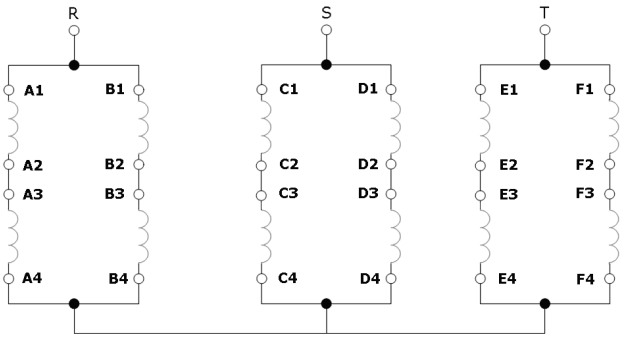

Figure 13 Scheme of healthy loaded synchronous motor

Measurements and analysis were carried out for 4 states of loaded synchronous motor (Fig. 10 ÷ 13). 2 training sets contained 8 5-second samples. Test set contained 100 5-second samples (25 samples of each state of loaded synchronous motor). On the basis of Tab. 1 SMOFS-25-EXPANDED selected frequencies 149, 168, 205 Hz and 149 Hz. Efficiency of recognition of acoustic signal was expressed by:

$$EoR = \frac{NoRTS}{NATS} 100\,\%, \tag{8}$$

where: EoR - the efficiency of recognition of acoustic signal, $NoRTS$ - the number of proper recognized test samples, $NATS$ - the number of all test samples in test set.

The total efficiency of recognition of acoustic signal ($TEoR$) was defined as:

$$TEoR = \frac{EoR_1 + EoR_2 + EoR_3 + EoR_4}{4}, \tag{9}$$

where: *TEoR* - the total efficiency of recognition of acoustic signal, EoR_1 - the efficiency of recognition of acoustic signal of healthy loaded synchronous motor, EoR_2 - the efficiency of recognition of acoustic signal of loaded synchronous motor with shorted stator coil (B1-B2), EoR_3 - the efficiency of recognition of acoustic signal of loaded synchronous motor with shorted stator coil (B1-B2) and broken coil (C2-C3), EoR_4 - the efficiency of recognition of acoustic signal of loaded synchronous motor with shorted stator coil (B1-B2) and two broken coils (C2-C3, E2-E3).

Table 2 Results of recognition of acoustic signal of loaded synchronous motor using SMOFS-25-EXPANDED and LDA

State of loaded synchronous motor	*TE* = 0,83	*TE* = 0,65
	EoR (%)	*EoR* (%)
Healthy loaded synchronous motor	100	100
Loaded synchronous motor with shorted stator coil (B1-B2)	100	100
Loaded synchronous motor with shorted stator coil (B1-B2) and broken coil (C2-C3)	92	92
Loaded synchronous motor with shorted stator coil (B1-B2) and two broken coils (C2-C3, E2-E3)	100	100
	TEoR (%)	*TEoR* (%)
4 analysed states of loaded synchronous motor	98	98

Table 3 Results of recognition of acoustic signal of loaded synchronous motor using SMOFS-25-EXPANDED and NN

State of loaded synchronous motor	*TE* = 0,83	*TE* = 0,65
	EoR (%)	*EoR* (%)
Healthy loaded synchronous motor	100	100
Loaded synchronous motor with shorted stator coil (B1-B2)	100	96
Loaded synchronous motor with shorted stator coil (B1-B2) and broken coil (C2-C3)	88	100
Loaded synchronous motor with shorted stator coil (B1-B2) and two broken coils (C2-C3, E2-E3)	96	100
	TEoR (%)	*TEoR* (%)
4 analysed states of loaded synchronous motor	96	99

Table 4 Results of recognition of acoustic signal of loaded synchronous motor using SMOFS-25-EXPANDED and SOM

State of loaded synchronous motor	*TE* = 0,83	*TE* = 0,65
	EoR (%)	*EoR* (%)
Healthy loaded synchronous motor	100	100
Loaded synchronous motor with shorted stator coil (B1-B2)	64	64
Loaded synchronous motor with shorted stator coil (B1-B2) and broken coil (C2-C3)	92	100
Loaded synchronous motor with shorted stator coil (B1-B2) and two broken coils (C2-C3, E2-E3)	76	92
	TEoR (%)	*TEoR* (%)
4 analysed states of loaded synchronous motor	83	89

The results of recognition of acoustic signals of loaded synchronous motor were presented in Tabs. 2 ÷ 4. The analysed efficiency of recognition of acoustic signal (*EoR*) was in the range of 92 ÷ 100 % (Tab. 2). The total efficiency of recognition of acoustic signal (*TEoR*) was equal to 98 % for SMOFS-25-EXPANDED and LDA.

EoR was in the range of 96 ÷ 100 % for *TE* = 0,65 (Tab. 3). *TEoR* was equal 99 % for *TE* = 0,65, SMOFS-25-EXPANDED and NN classifier.

EoR was in the range of 64 ÷ 100 % for *TE* = 0,65 (Tab. 4). *TEoR* was equal to 89 % for *TE* = 0,65, SMOFS-25-EXPANDED and SOM. Parameter *TE* = 0,65 gave higher value of *TEoR* than *TE* = 0,83 (Tab. 3, 4). The best results were obtained for *TE* = 0,65, SMOFS-25-EXPANDED and NN classifier (Tab. 3).

4 Conclusions

The feature extraction method called SMOFS-25-EXPANDED was presented in this paper. This method was applied to diagnostics of loaded synchronous motor. The proposed approach used acoustic signals produced by 4 analysed states of machine. Classifiers such as LDA, NN, SOM were analysed. The best results were obtained for parameter *TE* = 0,65, SMOFS-25-EXPANDED and NN classifier *TEoR* (total efficiency of recognition of acoustic signal) = 99 %.

Proposed approach is inexpensive, non-invasive and can be used to protect loaded synchronous motors. It can find application in other diagnostic methods related to other types of electric motors, engines and equipment consisting of rotating electric motors. In the future it can be also used with other fault detection methods based on electric and thermal signals. In this way more reliable methods of fault detection will be used in the industry.

Acknowledgements

The research has been supported by AGH University of Science and Technology, grant nr 11.11.120.612.

5 References

[1] Glowacz, Z.; Kozik, J. Detection of synchronous motor inter-turn faults based on spectral analysis of park's vector. // Archives of Metallurgy and Materials. 58, 1(2013), pp. 19-23. DOI: 10.2478/v10172-012-0144-y

[2] Krolczyk, G. M.; Nieslony, P.; Krolczyk, J. B.; Samardzic, I.; Legutko, S.; Hloch, S.; Barrans, S.; Maruda, RW. Influence of argon pollution on the weld surface morphology. // Measurement. 70 (2015), pp. 203-213. DOI: 10.1016/j.measurement.2015.04.001

[3] Barglik, J.; Smalcerz, A.; Smagor, A.; Paszek, P. Analysis of Continuous Induction Hardening of Steel Cylinder Element Made of Steel 38Mn6. // Archives of Metallurgy and Materials. 60, 4(2015), pp. 2861-2866. DOI: 10.1515/amm-2015-0457

[4] Tokarski, T.; Wzorek, L.; Dybiec, H. Microstructure and Plasticity of Hot Deformed 5083 Aluminum Alloy Produced by Rapid Solidification and Hot Extrusion. // Archives of Metallurgy and Materials. 57, 4(2012), pp. 1253-1259.

[5] Krolczyk, G. M.; Krolczyk, J. B.; Maruda, R. W.; Legutko, S.; Tomaszewski, M. Metrological changes in surface morphology of high-strength steels in manufacturing processes. // Measurement, 88 (2016), pp. 176-185. DOI: 10.1016/j.measurement.2016.03.055

[6] Zhao, Z.; Wang, C.; Zhang, Y. G.; Sun, Y. Latest progress of fault detection and localization in complex Electrical Engineering. // Journal of Electrical Engineering-

Elektrotechnicky Casopis. 65, 1(2014), pp. 55-59. DOI: 10.2478/jee-2014-0008
[7] Jiang Y.; Li Z. X.; Zhang C.; Hu C.; Peng Z. On the bi-dimensional variational decomposition applied to nonstationary vibration signals for rolling bearing crack detection in coal cutters. // Measurement Science and Technology. 27, 6(2016), Article Number: 065103. DOI: 10.1088/0957-0233/27/6/065103
[8] Glowacz, A.; Glowacz, W.; Glowacz, Z. Recognition of armature current of DC generator depending on rotor speed using FFT, MSAF-1 and LDA. // Eksploatacja i Niezawodnosc - Maintenance and Reliability. 17, 1(2015), pp. 64-69. DOI: 10.17531/ein.2015.1.9
[9] Glowacz, A.; Glowacz, A.; Glowacz, Z. Recognition of Monochrome Thermal Images of Synchronous Motor with the Application of Skeletonization and Classifier Based on Words. // Archives of Metallurgy and Materials. 60, 1(2015), pp. 27-32. DOI: 10.1515/amm-2015-0004
[10] Glowacz, W.; Glowacz, Z. Diagnostics of separately excited DC motor based on analysis and recognition of signals using FFT and Bayes classifier. // Archives of Electrical Engineering, 64, 1(2015), pp. 29-35. DOI: 10.1515/aee-2015-0004
[11] Glowacz, A. DC Motor Fault Analysis with the Use of Acoustic Signals, Coiflet Wavelet Transform, and K-Nearest Neighbor Classifier. // Archives of Acoustics. 40, 3(2015), pp. 321-327. DOI: 10.1515/aoa-2015-0035
[12] Delgado-Arredondo, P. A.; Garcia-Perez, A.; Morinigo-Sotelo, D.; Osornio-Rios, RA.; Avina-Cervantes, JG.; Rostro-Gonzalez, H.; Romero-Troncoso, RD. Comparative Study of Time-Frequency Decomposition Techniques for Fault Detection in Induction Motors Using Vibration Analysis during Startup Transient. // Shock and Vibration. Article Number: 708034, (2015). DOI: 10.1155/2015/708034
[13] Mika, D.; Jozwik, J. Normative measurements of noise at CNC machines work stations. // Advances in Science and Technology-Research Journal. 10, 30(2016), pp. 138-143. DOI: 10.12913/22998624/63387
[14] Jena, D. P.; Panigrahi, S. N. Automatic gear and bearing fault localization using vibration and acoustic signals. // Applied Acoustics. 98 (2015), pp. 20-33. DOI: 10.1016/j.apacoust.2015.04.016
[15] Michalak, M.; Sikora, B.; Sobczyk, J. Diagnostic Model for Longwall Conveyor Engines. // Man-Machine Interactions 4, ICMMI 2015, Book Series: Advances in Intelligent Systems and Computing. 391 (2016), pp. 437-448. DOI: 10.1007/978-3-319-23437-3_37
[16] Sawczuk, W. Application of vibroacoustic diagnostics to evaluation of wear of friction pads rail brake disc. // Eksploatacja i Niezawodnosc – Maintenance and Reliability. 18, 4(2016), pp. 565-571. DOI: 10.17531/ein.2016.4.11.
[17] Rzeszucinski, P.; Orman, M.; Pinto, C. T.; Tkaczyk, A.; Sulowicz, M. A signal processing approach to bearing fault detection with the use of a mobile phone. // 2015 IEEE 10th International Symposium on Diagnostics for Electric Machines, Power Electronics and Drives (SDEMPED), (2015), pp. 310-315.
[18] Pleban, D. Definition and Measure of the Sound Quality of the Machine. // Archives of Acoustics. 39, 1 (2014), pp. 17-23.
[19] Lara, R.; Jimenez-Romero, R.; Perez-Hidalgo, F.; Redel-Macias, M. D. Influence of constructive parameters and power signals on sound quality and airborne noise radiated by inverter-fed induction motors. // Measurement. 73 (2015), pp. 503-514, DOI: 10.1016/j.measurement.2015.05.049
[20] Baranski, M.; Decner, A.; Polak, A. Selected Diagnostic Methods of Electrical Machines Operating in Industrial Conditions. // IEEE Transactions on Dielectrics and Electrical Insulation. 21, 5(2014), pp. 2047-2054. DOI: 10.1109/TDEI.2014.004602
[21] Van Hecke, B.; Yoon, J.; He, D. Low speed bearing fault diagnosis using acoustic emission sensors. // Applied Acoustics. 105 (2016), pp. 35-44. DOI: 10.1016/j.apacoust.2015.10.028
[22] Li, Z. X.; Jiang, Y.; Hu, C.; Peng, Z. Recent progress on decoupling diagnosis of hybrid failures in gear transmission systems using vibration sensor signal: A review. // Measurement, 90 (2016), pp. 4-19. DOI: 10.1016/j.measurement.2016.04.036
[23] Jozwik, J. Identification and monitoring of noise sources of CNC machine tools by acoustic Holography methods. // Advances in Science and Technology-Research Journal, 10, 30(2016), pp. 127-137. DOI: 10.12913/22998624/63386
[24] Rusinski, E.; Moczko, P.; Odyjas, P.; Pietrusiak, D. Investigation of vibrations of a main centrifugal fan used in mine ventilation. // Archives of Civil and Mechanical Engineering. 14, 4(2014), pp. 569-579. DOI: 10.1016/j.acme.2014.04.003
[25] Ebrahimi, B. M.; Faiz, J. Diagnosis and performance analysis of three-phase permanent magnet synchronous motors with static, dynamic and mixed eccentricity. // IET Electric Power Applications. 4, 1(2010), pp. 53-66. DOI: 10.1049/iet-epa.2008.0308
[26] Koprowski, R. Some selected quantitative methods of thermal image analysis in Matlab. // Journal of Biophotonics. 9, 5(2016), pp. 510-520. DOI: 10.1002/jbio.201500224
[27] Liu, H.; Wang, Z. X.; Zhong, J.; Xie Z. W. Early detection of spontaneous combustion disaster of sulphide ore stockpiles. // Tehnicki Vjesnik-Technical Gazette. 22, 6(2015), pp. 1579-1587. DOI: 10.17559/TV-20150522125313
[28] Kulka, Z. Advances in Digitization of Microphones and Loudspeakers. // Archives of Acoustics. 36, 2(2011), pp. 419-436. DOI: 10.2478/v10168-011-0030-z
[29] MathWorks – MATLAB and SimuLink for Technical Computing 2015; www.mathworks.com.
[30] Dudek-Dyduch, E.; Tadeusiewicz, R.; Horzyk, A. Neural network adaptation process effectiveness dependent of constant training data availability. // Neurocomputing. 72, 13-15 (2009), pp. 3138-3149. DOI: 10.1016/j.neucom.2009.03.017
[31] Augustyniak, P.; Smolen, M.; Mikrut, Z.; Kantoch, E. Seamless Tracing of Human Behavior Using Complementary Wearable and House-Embedded Sensors. // Sensors. 14, 5(2014), pp. 7831-7856. DOI: 10.3390/s140507831
[32] Roj, J.; Cichy, A. Method of Measurement of Capacitance and Dielectric Loss Factor Using Artificial Neural Networks. // Measurement Science Review. 15, 3(2015), 127-131. DOI: 10.1515/msr-2015-0019
[33] Valis, D.; Pietrucha-Urbanik, K. Utilization of diffusion processes and fuzzy logic for vulnerability assessment. // Eksploatacja i Niezawodnosc–Maintenance and Reliability. 16, 1(2014), pp. 48-55.
[34] Glowacz, A.; Glowacz, A.; Glowacz, Z. Recognition of thermal images of direct current motor with application of area perimeter vector and Bayes classifier. // Measurement Science Review. 15, 3(2015), pp: 119-126. DOI: 10.1515/msr-2015-0018
[35] Deptula, A.; Osinski, P.; Radziwanowska, U. Decision Support System for Identifying Technical Condition of Combustion Engine. // Archives of Acoustics, 41, 3(2016), pp. 449-460.
[36] Kundegorski, M.; Jackson, P. J. B.; Ziolko, B. Two-Microphone Dereverberation for Automatic Speech Recognition of Polish. // Archives of Acoustics. 39, 3(2014), pp. 411-420.

[37] Czopek, K. Cardiac Activity Based on Acoustic Signal Properties. // Acta physica polonica A. 121, 1A(2012), pp. A42-A45. DOI: 10.12693/APhysPolA.121.A-42
[38] Rusek, K.; Orzechowski, T.; Dziech, A. LDA for Face Profile Detection. // 4th International Conference on Multimedia Communications, Services and Security (MCSS 2011). Book Series: Communications in Computer and Information Science. 149, (2011), 144-148.
[39] Alfons, C.; Fredäng, E.; Lind, P. Nearest Neighbor Classifiers. // TNM033 Data Mining Techniques, (2009-12-04).
[40] Chalasani, R.; Principe, J. C. Self-organizing maps with information theoretic learning. // Neurocomputing. 147 (2015), pp. 3-14. DOI: 10.1016/j.neucom.2013.12.059
[41] Olszewski, D. Fraud detection using self-organizing map visualizing the user profiles. // Knowledge-Based Systems. 70, Special Issue, (2014), pp. 324-334. DOI: 10.1016/j.knosys.2014.07.008
[42] Gorny, Z.; Kluska-Nawarecka, S.; Wilk-Kolodziejczyk, D.; Regulski, K. Methodology for the construction of a rule-based knowledge base enabling the selection of appropriate bronze heat treatment parameters using rough sets. // Archives of Metallurgy and Materials. 60, 1(2015), pp. 309–312. DOI: 10.1515/amm-2015-0050
[43] Glowacz, A. Recognition of acoustic signals of induction motor using FFT, SMOFS-10 and LSVM. // Eksploatacja i Niezawodnosc–Maintenance and Reliability. 17, 4(2015), pp. 569-574. DOI: 10.17531/ein.2015.4.12
[44] Panek, D.; Skalski, A.; Gajda, J.; Tadeusiewicz, R. Acoustic analysis assessment in speech pathology detection. // International Journal of Applied Mathematics and Computer Science. 25, 3(2015), pp. 631-643. DOI: 10.1515/amcs-2015-0046
[45] Jun, S.; Kochan, O. Investigations of Thermocouple Drift Irregularity Impact on Error of their Inhomogeneity Correction. // Measurement Science Review. 14, 1(2014), pp. 29-34.
[46] Deptula, A.; Kunderman, D.; Osinski, P.; Radziwanowska, U.; Wlostowski, R. Acoustic Diagnostics Applications in the Study of Technical Condition of Combustion Engine. // Archives of Acoustics. 41, 2(2016), pp. 345-350. DOI: 10.1515/aoa-2016-0036
[47] Hachaj, T. Pattern Classification Methods for Analysis and Visualization of Brain Perfusion CT Maps. // Computational Intelligence Paradigms in Advanced Pattern Classification, Book Series: Studies in Computational Intelligence, 386 (2012), pp. 145–170.
[48] Jaworek-Korjakowska, J.; Kleczek, P. Automatic Classification of Specific Melanocytic Lesions Using Artificial Intelligence. // BioMed Research International, Article Number: 8934242, (2016). DOI: 10.1155/2016/8934242
[49] Khan, Z. F.; Kannan, A. Intelligent Segmentation of Medical Images using Fuzzy Bitplane Thresholding. // Measurement Science Review. 14, 2(2014), pp. 94-101. DOI: 10.2478/msr-2014-0013
[50] Glowacz, A. Diagnostics of Rotor Damages of Three-Phase Induction Motors Using Acoustic Signals and SMOFS-20-EXPANDED. // Archives of Acoustics. 41, 3(2016), pp. 507-515.
[51] Glowacz, A. Recognition of Acoustic Signals of Synchronous Motors with the Use of MoFS and Selected Classifiers. // Measurement Science Review. 15, 4(2015), pp. 167-175. DOI: 10.1515/msr-2015-0024
[52] Jia, F.; Lei, Y. G.; Lin, J.; Zhou, X.; Lu, N. Deep neural networks: A promising tool for fault characteristic mining and intelligent diagnosis of rotating machinery with massive data. // Mechanical Systems and Signal Processing. 72-73 (2016), pp. 303-315. DOI: 10.1016/j.ymssp.2015.10.025
[53] Yadav, A.; Swetapadma, A. A novel transmission line relaying scheme for fault detection and classification using wavelet transform and linear discriminant analysis. // Ain Shams Engineering Journal. 6, 1(2015), pp. 199-209. DOI: 10.1016/j.asej.2014.10.005
[54] Marzec, M.; Koprowski, R.; Wrobel, Z. Methods of face localization in thermograms. // Biocybernetics and Biomedical Engineering. 35, 2 (2015), pp: 138-146. DOI: 10.1016/j.bbe.2014.09.001
[55] Swedrowski, L.; Duzinkiewicz, K.; Grochowski, M.; Rutkowski, T. Use of neural networks in diagnostics of rolling-element bearing of the induction motor. // Smart Diagnostics V, Book Series: Key Engineering Materials. 588, (2014), pp. 333-342.
[56] Glowacz, Z. Automatic Recognition of Armature Current of DC Motor with Application of FFT and GSDM. // Archives of Metallurgy and Materials. 56, 1(2011), pp. 25-30. DOI: 10.2478/v10172-011-0003-2
[57] Jun, S.; Kochan, O.; Kochan, V.; Wang, C. Z. Development and Investigation of the Method for Compensating Thermoelectric Inhomogeneity Error. // International Journal of Thermophysics. 37, 1(2016). Article Number: 10. DOI: 10.1007/s10765-015-2025-x

Author address

Adam Glowacz, Assistant Prof. Dr.
AGH University of Science and Technology,
Faculty of Electrical Engineering, Automatics,
Computer Science and Biomedical Engineering,
Department of Automatics and Biomedical Engineering,
al. A. Mickiewicza 30, 30-059 Krakow, Poland
E-mail: adglow@agh.edu.pl